# Chapter 2
# On the Use of Analytical Methods in Electromagnetic Compatibility and Magnetohydrodynamics

**Silvestar Šesnić and Dragan Poljak**

**Abstract** The paper deals with the use of analytical methods for solving various integro-differential equations in electromagnetic compatibility, with the emphasis on the frequency and time domain solutions of the thin wire configurations buried in a lossy ground. Solutions in the frequency domain are carried out via certain mathematical manipulations with the current function appearing in corresponding integral equations. On the other hand, analytical solutions in the time domain are undertaken using the Laplace transform and Cauchy residue theorem. Obtained analytical results are compared to those calculated using the numerical solution of the frequency domain Pocklington equation, where applicable. Also, an overview of analytical solutions to the Grad–Shafranov equation for tokamak plasma is given.

**Keywords** Electromagnetic compatibility · Thin wire analysis · Integro-differential equations · Analytical methods · Magnetohydrodynamics

## 2.1 Introduction

The electromagnetic field coupling to thin wire scatterers can be treated either in frequency (FD) or time domain (TD) [18]. The principal advantage of the frequency domain approach is relative simplicity of both the formulation and the selected numerical treatment. However, time domain modeling ensures better physical insight, accurate modeling of highly resonant structures, possibility of calculating only early time period and easier implementation of nonlinearities [12, 21].

S. Šesnić (✉)
Department of Power Engineering, University of Split, FESB,
R. Boskovica 32, 21000 Split, Croatia
e-mail: ssesnic@fesb.hr

D. Poljak
Department of Electronics, University of Split, FESB,
R. Boskovica 32, 21000 Split, Croatia
e-mail: dpoljak@fesb.hr



S. Silvestrov and M. Rančić (eds.), *Engineering Mathematics I*,
Springer Proceedings in Mathematics & Statistics 178,
DOI 10.1007/978-3-319-42082-0_2

The formulation of the problem in thin wire analysis (FD or TD) is usually based on some variants of integral or integro-differential equation (Hallén or Pocklington type), respectively. Numerical modeling is widely used for solving various complex problems. On the other hand, analytical solution can be obtained when dealing with canonical problems, using a carefully chosen set of approximations [10, 26]. The advantage of analytical solutions over numerical ones is the ability to "follow up" the procedure with the complete control of adopted approximations. In this way, the insight into the physical characteristics of the problem is ensured, which is, when using numerical methods, rather complex task. Also, analytical solutions are readily implemented for benchmark purposes, as well as some fast engineering estimation of phenomena.

Valuable contributions in the area of analytical solutions of integral equations in electromagnetics are given by R.W.P. King *et al.* [9, 10]. S. Tkachenko derives the analytical solution for the current induced along the wire above perfectly conducting (PEC) ground using the transmission line modeling (TLM) for LF excitations [25]. On the other hand, time domain analytical modeling is not investigated to a greater extent and papers on the subject are rather scarce. A. Hoorfar and D. Chang give the solution for transient response of thin wire in free space using singularity expansion method [8]. R. Velazquez and D. Mukhedar derive analytical solution for the current induced along a grounding electrode, based on the TL model [27]. Analytical solutions in time domain have been reported by the authors in [20–22].

Analytical solutions pertaining to the mathematical model of fusion plasma, given by the set of magnetohydrodynamic (MHD) equations provide a satisfactory description of macroscopic plasma behavior. Combining MHD equations with Maxwell's equations of classical electrodynamics yields nonlinear second order differential equation known as Grad–Shafranov equation (GSE) [1]. Analytical solutions of the GSE are very useful for theoretical studies of plasma equilibrium, transport and MHD stability [28].

## 2.2 Thin Wire Models in Antenna Theory

### *2.2.1 Frequency Domain Formulation*

Horizontal, perfectly conducting wire of length $L$ and radius $a$, embedded in a lossy medium at depth $d$ and excited by a plane wave is considered, as shown in Fig. 2.1. The medium is characterized with electric permittivity $\varepsilon$ and conductivity $\sigma$. Dimensions of the structure satisfy the thin-wire approximation [12].

The current induced along the wire is governed by the inhomogeneous Pocklington integro-differential equation [17]

$$-\frac{1}{j4\pi\omega\varepsilon_{eff}}\left(\frac{\partial^2}{\partial x^2}-\gamma^2\right)\int_0^L I\left(x'\right)g\left(x,x'\right)dx'=E_x\left(\omega\right), \tag{2.1}$$

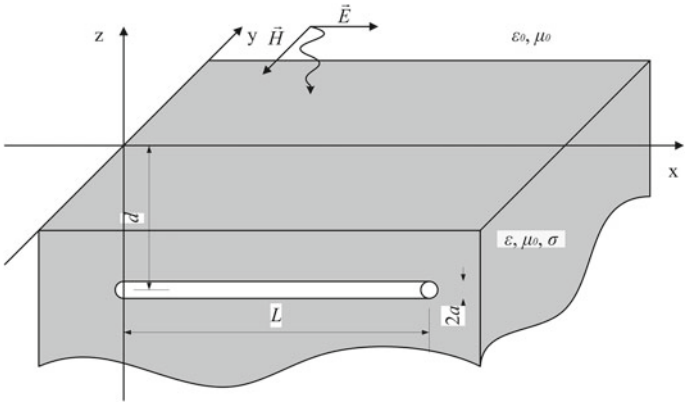


**Fig. 2.1** Horizontal *straight thin wire* buried in a lossy medium

where $I\left(x'\right)$ denotes current distribution along the wire. Complex permittivity of the medium is defined as

$$\varepsilon_{eff} = \varepsilon_r \varepsilon_0 - j\frac{\sigma}{\omega}, \tag{2.2}$$

where $\varepsilon_r$ and $\sigma$ represent relative electric permittivity and conductivity, respectively. Green's function $g\left(x, x'\right)$ can be expressed as [14]

$$g\left(x, x'\right) = g_0\left(x, x'\right) - \Gamma_{ref}\, g_i\left(x, x'\right), \tag{2.3}$$

where $g_0\left(x, x'\right)$ denotes the lossy medium Green's function

$$g_0\left(x, x'\right) = \frac{e^{-\gamma R_1}}{R_1}, \tag{2.4}$$

and $g_i\left(x, x'\right)$ is Green's function according to the image theory

$$g_i\left(x, x'\right) = \frac{e^{-\gamma R_2}}{R_2}. \tag{2.5}$$

Propagation constant of the medium is defined in the following way

$$\gamma = \sqrt{j\omega\mu\sigma - \omega^2\mu\varepsilon}, \tag{2.6}$$

and distances $R_1$ and $R_2$ correspond to distances from the source and the image to the observation point, respectively

$$R_1 = \sqrt{(x - x')^2 + a^2},$$
$$R_2 = \sqrt{(x - x')^2 + 4d^2}. \tag{2.7}$$

Presence of the earth-air interface is taken into account via the reflection coefficient within the Green's function (2.3). The reflection coefficient can be taken in the form of Fresnel coefficient [3, 5] or, as a simpler solution, from Modified Image Theory (MIT) [23]. The Fresnel reflection coefficient is considered to be better approximation of the Sommerfeld theory [11] and is defined as

$$\Gamma_{ref}^{Fr} = \frac{\frac{1}{\underline{n}}\cos\theta - \sqrt{\frac{1}{\underline{n}} - \sin^2\theta}}{\frac{1}{\underline{n}}\cos\theta + \sqrt{\frac{1}{\underline{n}} - \sin^2\theta}},$$
$$\theta = arctg\frac{|x - x'|}{2d},\ \underline{n} = \frac{\varepsilon_{eff}}{\varepsilon_0}. \tag{2.8}$$

On the other hand, the reflection coefficient that arises from MIT is defined as follows [23]

$$\Gamma_{ref}^{MIT} = -\frac{\varepsilon_{eff} - \varepsilon_0}{\varepsilon_{eff} + \varepsilon_0}. \tag{2.9}$$

The scattered voltage along the wire is defined as an integral of the vertical component of the scattered electric field and the Generalized Telegrapher's Equation for spatial distribution of the scattered voltage is given as [16]

$$V^{sct}(x) = -\frac{1}{j4\pi\omega\varepsilon_{eff}}\int_0^L \frac{\partial I(x')}{\partial x'} g(x, x')\, dx', \tag{2.10}$$

which can be easily determined, once the current distribution is known.

### 2.2.2 Time Domain Formulation

In the case of time domain formulation, the same configuration is considered as shown in Fig. 2.1 [7]. Governing equation for the unknown transient current flowing along the electrode is given in the form of time domain Pocklington integro-differential equation [21]

$$-\left(\frac{\partial^2}{\partial x^2} - \mu\sigma\frac{\partial}{\partial t} - \mu\varepsilon\frac{\partial^2}{\partial t^2}\right)\cdot\left[\frac{\mu}{4\pi}\int_0^L I\left(x', t - \frac{R}{v}\right)\frac{e^{-\frac{1}{\tau_g}\frac{R}{v}}}{R}dx' - \right.$$
$$\left. -\frac{\mu}{4\pi}\int_0^t\int_0^L \Gamma_{ref}^{MIT}(\tau)\, I\left(x', t - \frac{R^*}{v} - \tau\right)\frac{e^{-\frac{1}{\tau_g}\frac{R^*}{v}}}{R^*}dx'd\tau\right] = \left(\mu\varepsilon\frac{\partial}{\partial t} + \mu\sigma\right)E_x^{tr}(t), \tag{2.11}$$

where $I\left(x', t - \frac{R}{v}\right)$ represents the unknown transient current. Detailed derivation of (2.11) can be found in [21].

The distance from the source point in the wire axis to the observation point on the wire surface is given by

$$R = \sqrt{(x - x')^2 + a^2}, \tag{2.12}$$

while the distance from the source point on the image wire, according to the image theory is

$$R^* = \sqrt{(x - x')^2 + 4d^2}. \tag{2.13}$$

Time constant and propagation velocity in the lossy medium are defined as follows [21]

$$\begin{aligned} \tau_g &= \frac{2\varepsilon}{\sigma}, \\ v &= \frac{1}{\sqrt{\mu\varepsilon}}. \end{aligned} \tag{2.14}$$

The reflection coefficient arising from the Modified Image Theory is given by inverse Laplace transform of (2.9) [23]

$$\Gamma_{ref}^{MIT}(t) = -\left[\frac{\tau_1}{\tau_2}\delta(t) + \frac{1}{\tau_2}\left(1 - \frac{\tau_1}{\tau_2}\right)e^{-\frac{t}{\tau_2}}\right], \tag{2.15}$$

where

$$\begin{aligned} \tau_1 &= \frac{\varepsilon_0(\varepsilon_r - 1)}{\sigma}, \\ \tau_2 &= \frac{\varepsilon_0(\varepsilon_r + 1)}{\sigma}. \end{aligned} \tag{2.16}$$

Reflection coefficient (2.15) represents the simplest characterization of the earth-air interface, taking into account only medium properties. However, an extensive investigation of this coefficient applied to thin wires in two-media configuration has been carried out in [15].

## 2.3 Frequency Domain Applications of Analytical Methods

### *2.3.1 Horizontal Wire Below Ground*

To solve the Pocklington equation (2.1) analytically, the integral on the left-hand side of (2.1) can be written in the following manner [20]:

$$\int_0^L I\left(x'\right) g\left(x, x'\right) dx' = I(x) \int_0^L g\left(x, x'\right) dx' + \int_0^L \left[I(x') - I(x)\right] g\left(x, x'\right) dx'. \tag{2.17}$$

The integral on the left hand side can be approximated by the first term on the right hand side of (2.17), thus neglecting the second integral. Furthermore, the characteristic integral term over the Green function is evaluated analytically. For the case of an imperfectly conducting ground the appropriate analytical integration of the first integral on the right hand side of (2.17) gives [25]

$$\int_0^L g\left(x, x'\right) dx' = \psi = 2\left(\ln\frac{L}{a} - \Gamma_{ref}^{MIT} \ln\frac{L}{2d}\right), \tag{2.18}$$

where reflection coefficient is given with (2.9).

After performing some mathematical manipulations, the analytical solution (2.1) can be obtained in the closed form and is given by

$$I\left(x, \omega\right) = \frac{4\pi e^{j\frac{a}{v}\omega}}{j\omega\mu\Psi\left(\omega\right)} E_x^{exc}\left(\omega\right)\left[1 - \frac{\cosh\left(\gamma\left(\frac{L}{2} - x\right)\right)}{\cosh\left(\gamma\frac{L}{2}\right)}\right]. \tag{2.19}$$

Figures 2.2 and 2.3 are related to horizontal wire of length $L$, radius $a = 0.01\,\text{m}$, buried at depth $d = 2.5\,\text{m}$ in a lossy ground and illuminated by the plane wave of normal incidence transmitted into the ground with amplitude $E_0 = 1\,\text{V/m}$ at the interface between two media. Absolute value of spatial current distribution for lines $L = 5\,\text{m}$ and $L = 10\,\text{m}$. The operating frequency of $f = 50\,\text{MHz}$ is shown. The conductivity

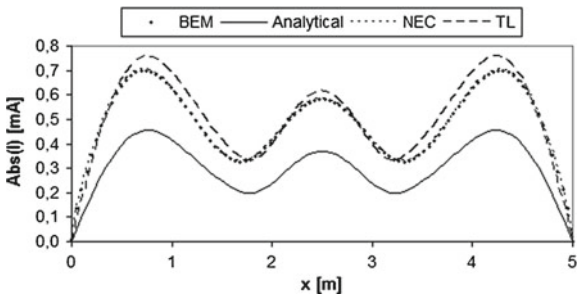


**Fig. 2.2** Absolute value of current distribution along the single wire buried in a ground, $L = 5\,\text{m}$

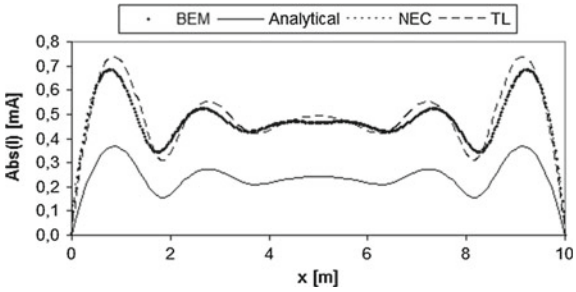


**Fig. 2.3** Absolute value of current distribution along the single wire buried in a ground, $L = 10\,\text{m}$

of the ground is $\sigma = 0.01\,\text{S/m}$ and permittivity is $\varepsilon_r = 10$. The agreement between results obtained via different methods (analytical and numerical) is satisfactory.

### 2.3.2 Horizontal Grounding Electrode

When horizontal grounding electrode is considered, (2.1) can be written as a homogeneous equation, since source function is incorporated through the boundary condition [20]

$$-\frac{1}{j4\pi\omega\varepsilon_{eff}}\left(\frac{\partial^2}{\partial x^2}-\gamma^2\right)\int_0^L I\left(x'\right)g\left(x,x'\right)dx'=0. \tag{2.20}$$

Now, the similar approach as in the case of horizontal wire can be adopted and (2.20) can be written as

$$-\frac{1}{j4\pi\omega\varepsilon_{eff}}\left(\frac{\partial^2}{\partial x^2}-\gamma^2\right)I\left(x\right)\int_0^L g\left(x,x'\right)dx'=0. \tag{2.21}$$

Integral in (2.21) can be readily calculated as given in [20]

$$\int_0^L g\left(x,x'\right)dx'=2\left(\ln\frac{L}{a}-\Gamma_{ref}\ln\frac{L}{2d}\right)=\Psi. \tag{2.22}$$

Now, the homogeneous Pocklington equation (2.21) simplifies into

$$\left(\frac{\partial^2}{\partial x^2}-\gamma^2\right)I\left(x\right)=0. \tag{2.23}$$

Equation (2.23) is readily solved and the solution is given with

$$I\left(x\right)=I_g\frac{\sinh\left[\gamma\left(L-x\right)\right]}{\sinh\left(\gamma L\right)}. \tag{2.24}$$

The expression for scattered voltage can be obtained substituting (2.24) into (2.10), which yields

$$V^{sct}(x) = \frac{\gamma I_g}{j4\pi\omega\varepsilon_{eff}\sinh(\gamma L)} \int_0^L \cosh\left[\gamma(L-x)\right] g\left(x, x'\right) dx'. \tag{2.25}$$

Integral in (2.25) is computed by means of standard numerical integration.

In Fig. 2.4, the current distribution along the electrode $L = 10\,\text{m}$, buried at $d = 0.3\,\text{m}$, with ground properties $\sigma = 0.01\,\text{S/m}$ and $\varepsilon_r = 10$ at the operating frequency $f = 10\,\text{MHz}$. The waveforms obtained via different approaches are very similar.

Figure 2.5 shows the results for transient impedance of an electrode of $L = 10\,\text{m}$, buried in a ground of conductivity $\sigma = 1\,\text{mS/m}$ for $1/10\,\mu\text{s}$ lightning pulse. It can be seen that the agreement between analytical and numerical results is very good, except for the early time response where discrepancy of around 10 % can be observed.

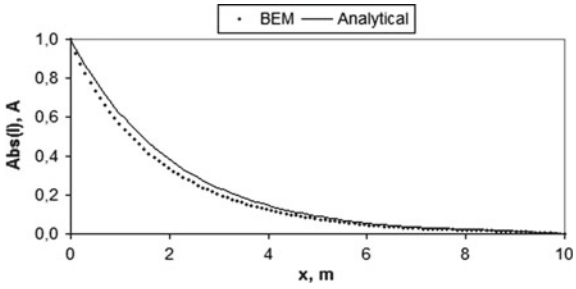


**Fig. 2.4** Absolute value of a current distribution along the horizontal electrode

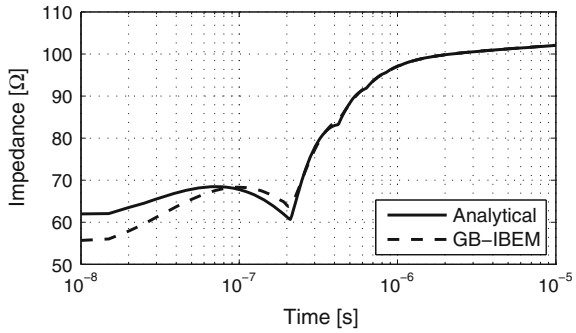


**Fig. 2.5** Transient impedance of the grounding electrode

## 2.4 Time Domain Applications of Analytical Methods

### 2.4.1 Horizontal Wire Below Ground

To obtain analytical solution of (2.11), the integral operator is simplified, using addition and subtraction technique

$$\int_0^L I\left(x', t-\frac{R}{v}\right)\frac{e^{-\frac{1}{\tau_g}\frac{R}{v}}}{R}dx' = I\left(x, t-\frac{a}{v}\right)\int_0^L \frac{e^{-\frac{1}{\tau_g}\frac{R}{v}}}{R}dx'. \tag{2.26}$$

This approximation has proven to be valid in papers by Tijhuis *et al.* [4, 24]. Next step in solving the differential equation (2.11) is to apply the Laplace transform and obtain the following equation

$$\left(\mu\varepsilon s+\mu\sigma\right)E_x^{tr}(s) = -\frac{\mu}{4\pi}\left(\frac{\partial^2}{\partial x^2}-\mu\sigma s-\mu\varepsilon s^2\right)\cdot$$
$$\cdot I(x,s)\,e^{-\frac{a}{v}s}\left[\int_0^L \frac{e^{-\frac{1}{\tau_g}\frac{R}{v}}}{R}dx' - \Gamma_{ref}^{MIT}(s)\int_0^L \frac{e^{-\frac{1}{\tau_g}\frac{R^*}{v}}}{R^*}dx'\right]. \tag{2.27}$$

Integrals in (2.27) can be solved analytically as follows [25]

$$\Psi(s) = \int_0^L \frac{e^{-\frac{1}{\tau_g}\frac{R}{v}}}{R}dx' - \Gamma_{ref}^{MIT}(s)\int_0^L \frac{e^{-\frac{1}{\tau_g}\frac{R^*}{v}}}{R^*}dx' = 2\left(\ln\frac{L}{a}+\frac{s\tau_1+1}{s\tau_2+1}\ln\frac{L}{2d}\right). \tag{2.28}$$

Now, relation (2.27) can be written as

$$\frac{\partial^2 I(x,s)}{\partial x^2}-\gamma^2 I(x,s) = -\frac{4\pi}{\mu s\Psi(s)}e^{\frac{a}{v}s}\gamma^2 E_x^{tr}(s). \tag{2.29}$$

The solution of (2.29) can be readily obtained, prescribing the boundary conditions at the wire ends

$$I(0,s)=0,$$
$$I(L,s)=0. \tag{2.30}$$

The solution of (2.29) is written as

$$I(x,s) = \frac{4\pi e^{\frac{a}{v}s}}{\mu s\Psi(s)}E_x^{tr}(s)\left[1-\frac{\cosh\left(\gamma\left(\frac{L}{2}-x\right)\right)}{\cosh\left(\gamma\frac{L}{2}\right)}\right]. \tag{2.31}$$

To obtain the solution for the current distribution in time domain, inverse Laplace transform has to be performed featuring the Cauchy residue theorem [19]

$$f(t) = \lim_{y\to\infty} \frac{1}{j2\pi} \int_{x-jy}^{x+jy} e^{ts} F(s)\, ds = \sum_{k=1}^{n} \mathrm{Res}\,(s_k)\,. \tag{2.32}$$

Calculating all the residues of the function (2.31) and undertaking the inverse transform as in (2.32), the following expression is obtained

$$I(x,t) = \frac{4\pi}{\mu} \left\{ \begin{array}{l} R(s_\Psi) \left[1 - \frac{\cosh\left(\gamma_\Psi\left(\frac{L}{2}-x\right)\right)}{\cosh\left(\gamma_\Psi \frac{L}{2}\right)}\right] e^{\left(t+\frac{a}{v}\right)s_\Psi} - \\ -\frac{\pi}{\mu\varepsilon L^2} \sum_{n=1}^{\infty} \frac{2n-1}{\pm\sqrt{b^2-4c_n s_{1,2n}\Psi\left(s_{1,2n}\right)}} \sin\frac{(2n-1)\pi x}{L} e^{\left(t+\frac{a}{v}\right)s_{1,2n}} \end{array} \right\}, \tag{2.33}$$

where coefficients $R(s_\Psi)$ and $s_\Psi$ represent physical properties of the system

$$R(s_\Psi) = \frac{1}{2\ln\frac{L}{2d}\frac{s_\Psi}{s_\Psi\tau_2+1}\left(\tau_1 - \tau_2\frac{s_\Psi\tau_1+1}{s_\Psi\tau_2+1}\right)}, \quad s_\Psi = -\frac{\ln\frac{L}{a}+\ln\frac{L}{2d}}{\tau_1\ln\frac{L}{a}+\tau_2\ln\frac{L}{2d}}. \tag{2.34}$$

Furthermore, other coefficients in relation (2.33) are given as follows

$$\begin{aligned} \gamma_\Psi &= \sqrt{\mu\varepsilon\left(s_\Psi^2 + b s_\Psi\right)}, \\ s_{1,2n} &= \frac{1}{2}\left(-b \pm \sqrt{b^2-4c_n}\right), \\ b = \frac{\sigma}{\varepsilon}, \quad c_n &= \frac{(2n-1)^2\pi^2}{\mu\varepsilon L^2}, \quad n = 1, 2, 3, \ldots\,. \end{aligned} \tag{2.35}$$

Expression (2.33) represents the space-time distribution of the current along the straight wire buried in a lossy medium excited by an impulse excitation.

Furthermore, the response to an arbitrary excitation can be obtained performing the corresponding convolution. The excitation function is plane wave in the form of double exponential electromagnetic pulse tangential to the wire [16]

$$E_x(t) = E_0\left(e^{-\alpha t} - e^{-\beta t}\right). \tag{2.36}$$

In Fig. 2.6, transient current at the center of the straight wire with $L = 1\,\mathrm{m}$, $d = 30\,\mathrm{cm}$, $\sigma = 10\,\mathrm{mS/m}$ is shown. Relatively good agreement between the results is achieved for a short wire and higher conductivity of a medium.

Figure 2.7 shows the transient current induced at the center of straight longer wires buried in a lossy medium with $\sigma = 1\,\mathrm{mS/m}$. For a 10 m–long wire the agreement between the results is rather satisfactorily.

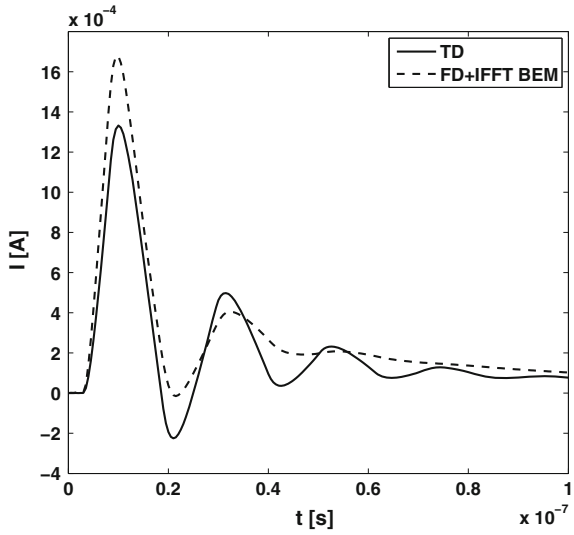


**Fig. 2.6** Transient current at the center of the straight wire, $L = 1\,\text{m}$, $d = 30\,\text{cm}$, $\sigma = 10\,\text{m S/m}$

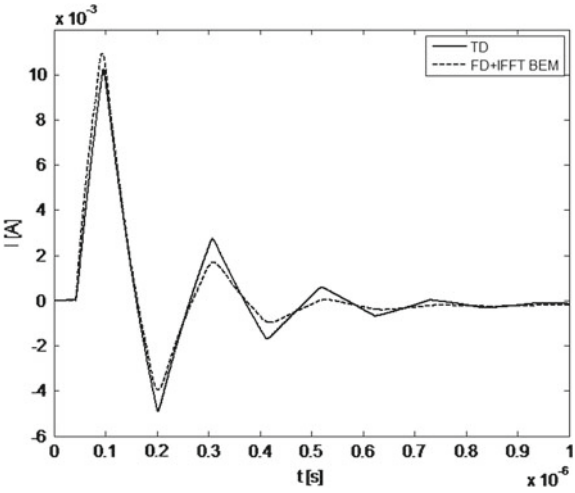


**Fig. 2.7** Transient current at the center of the straight wire, $L = 10\,\text{m}$, $d = 4\,\text{m}$, $\sigma = 1\,\text{m S/m}$

### 2.4.2 *Horizontal Grounding Electrode*

Homogeneous variant of integro-differential equation (2.11), representing the governing equation for grounding electrode can be solved analytically, as it has been reported recently by the authors in [22]. The governing equation (2.11) is simplified using (2.26). Now (2.11) can be written as follows

$$\frac{\partial^2 I(x,s)}{\partial x^2} - \gamma^2 I(x,s) = 0. \tag{2.37}$$

Prescribing the boundary conditions at the wire ends

$$I(0,s) = I_g(s), \qquad I(L,s) = 0, \tag{2.38}$$

the solution of (2.37) is readily obtained in the form

$$I(x,s) = I_g(s)\frac{\sinh\left[\gamma(L-x)\right]}{\sinh(\gamma L)}. \tag{2.39}$$

To obtain the solution for the current distribution in the time domain, inverse Laplace transform is performed and Cauchy residue theorem is applied [19] using (2.32). Having determined the residues of (2.39), the time domain counterpart is given

$$I(x,t) = \frac{2\pi}{\mu\varepsilon L^2}\sum_{n=1}^{\infty}\frac{(-1)^{n-1}n}{\pm\sqrt{b^2-4c_n}}\sin\frac{n\pi(L-x)}{L}e^{ts_{1,2n}}, \tag{2.40}$$

where corresponding coefficients are

$$s_{1,2n} = \frac{1}{2}\left(-b \pm \sqrt{b^2-4c_n}\right), \qquad b = \frac{\sigma}{\varepsilon}, \quad c_n = \frac{n^2\pi^2}{\mu\varepsilon L^2}, \quad n = 1,2,3,\ldots. \tag{2.41}$$

Equation (2.40) represents an analytical expression for the space-time distribution of the current flowing along the grounding electrode excited by an equivalent current source in the form of the Dirac pulse. On the other hand, one of the functions most frequently used to represent the lightning current is the double exponential pulse, given with [13]

$$I_g(t) = I_0\left(e^{-\alpha t} - e^{-\beta t}\right). \tag{2.42}$$

Analytical convolution is undertaken with (2.40) and (2.42), to obtain the expression for the current flowing along the electrode

$$I(x,t) = \frac{2\pi I_0}{\mu\varepsilon L^2}\sum_{n=1}^{\infty}\frac{(-1)^{n-1}n}{\pm\sqrt{b^2-4c_n}}\sin\frac{n\pi(L-x)}{L}\cdot \cdot\left(\frac{e^{s_{1,2n}t}-e^{-\alpha t}}{s_{1,2n}+\alpha} - \frac{e^{s_{1,2n}t}-e^{-\beta t}}{s_{1,2n}+\beta}\right). \tag{2.43}$$

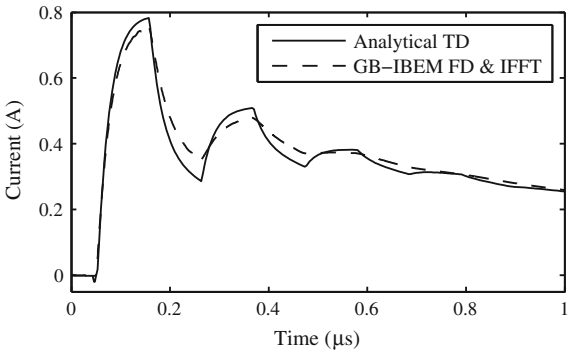


**Fig. 2.8** Transient current at the center of the grounding electrode, 0.1/1 $\mu$s pulse

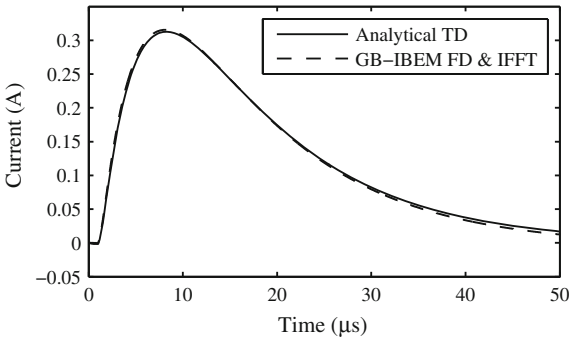


**Fig. 2.9** Transient current at the center of the grounding electrode, 1/10 $\mu$s pulse

Equation (2.43) represents the expression for the space-time distribution of the current flowing along the electrode due to a double exponential current source excitation.

Analytical results for the transient current induced at the center of the electrode are calculated with (2.43) and are compared to the results obtained via numerical approach. The results shown in Fig. 2.8 are calculated for the grounding electrode with $L = 10\,\text{m}$, buried in a lossy ground with the conductivity $\sigma = 1\,\text{mS/m}$. The agreement between the results is very good.

The results shown in Fig. 2.9 are related to calculations performed for electric properties of the ground $\sigma = 0.833\,\text{mS/m}$ and $\varepsilon_r = 9$. It is worth emphasizing that low ground conductivity is considered. The electrode is buried at depth $d = 0.5\,\text{m}$. Length of the grounding electrode is $L = 200\,\text{m}$. The agreement between analytical and numerical results for the current induced at the center of the electrodes is very good, especially for the longer electrode.

## 2.5 Some Analytical Solutions to the Grad–Shafranov Equation

Grad–Shafranov equation describing the plasma equilibrium is given as [28]

$$\frac{\partial^2\psi}{\partial r^2} - \frac{1}{r}\frac{\partial\psi}{\partial r} + \frac{\partial^2\psi}{\partial z^2} = -f\frac{df}{d\psi} - \mu_0 r^2\frac{dP}{d\psi}. \tag{2.44}$$

Various analytical solutions of GSE have been derived so far [6]. The analytical solutions are essential in describing various parameters that are involved in real tokamak scenarios as they are well suited for benchmarking various numerical codes. In this section, four different analytical solutions will be presented, with a short overview of their derivation as well as the emphasis to their applications.

### *2.5.1 Solution of the Homogeneous Equation*

In order to obtain any solution corresponding to the realistic source functions that appear on the right-hand side of (2.44), it is necessary to define possible solutions of the homogeneous equation given by

$$\frac{\partial^2\psi}{\partial r^2} - \frac{1}{r}\frac{\partial\psi}{\partial r} + \frac{\partial^2\psi}{\partial z^2} = 0. \tag{2.45}$$

Solution of (2.45) can be obtained by variable separation and is given with

$$\psi_0(r,z) = \left(c_1 r J_1(kr) + c_2 r Y_1(kr)\right)\left(c_3 e^{kz} + c_4 e^{-kz}\right). \tag{2.46}$$

On the other hand, the solutions can also be based on the series expansion [28]

$$\psi_0 = \sum_{n=0,2,\ldots} f_n(r)\, z^n. \tag{2.47}$$

One of the possible solutions satisfying these conditions and suitable for further implementation is [28]

$$\psi_0(r,z) = c_1 + c_2 r^2 + c_3\left(r^4 - 4r^2z^2\right) + c_4\left(r^2\ln r - z^2\right). \tag{2.48}$$

### 2.5.2 The Solov'ev Equilibrium

The Solov'ev equilibrium is the simplest usable solution to the inhomogeneous GSE [6]. It has been widely used in studies of plasma equilibrium, transport and MHD stability analysis.

The source functions in Solov'ev equilibrium are linear in $\psi$ and are given as [2]

$$P(\psi) = \frac{A}{\mu_0}\psi, \quad f^2(\psi) = 2B\psi + F_0^2, \tag{2.49}$$

with the corresponding solution

$$\psi(r,z) = \psi_0(r,z) - \frac{A}{8}r^4 - \frac{B}{2}z^2. \tag{2.50}$$

Wide variety of plasma shapes can be generated using (2.50). However, the current profile of this solution is restricted, since implementation of $A$ and $B$ allow choosing only two plasma parameters.

### 2.5.3 The Herrnegger–Maschke Solutions

The solution to the GSE for a parabolic source functions was reported in [6]

$$P(\psi) = \frac{C}{2\mu_0}\psi^2, \quad f^2(\psi) = D\psi^2 + F_0^2. \tag{2.51}$$

The solution of (2.51) can be given in the form of Coulomb wave functions as [2]

$$\psi = \alpha\left(F_0(\eta,x) + \gamma G_0(\eta,x)\right)\cos(kz). \tag{2.52}$$

As is the case for the Solov'ev equilibrium, the Herrnegger–Maschke solutions have only two free parameters, namely $C$ and $D$, which allow independent specification of plasma current and pressure ratio.

### 2.5.4 Mc Carthy's Solution

Innovative source functions were introduced by Mc Carthy in [6]. These source functions are dissimilar in their nature and describes a linear dependence of pressure and quadratic dependence of the current profile

$$P(\psi) = \frac{S}{\mu_0}\psi, \quad f^2(\psi) = T\psi^2 + 2U\psi + F_0^2. \tag{2.53}$$

Equation (2.53) can be solved by the separation of variables where the following equations are obtained

$$\frac{\partial^2 H(z)}{\partial z^2} + k^2 H(z) = 0, \tag{2.54}$$

$$\frac{\partial^2 G(r)}{\partial r^2} - \frac{1}{r}\frac{\partial G(r)}{\partial r} - \left(k^2 - T\right) G(r) = 0. \tag{2.55}$$

The solution for $H(z)$ is readily obtained as

$$H(z) = c_1 e^{jkz} + c_2 e^{-jkz}, \tag{2.56}$$

while the solution of (2.55) is given with

$$G(r) = rB_1(ar), \tag{2.57}$$

where $B_1$ denotes the family of Bessel functions and parameter $a$ satisfies the equation [6]

$$a^2 = \pm\left(T - k^2\right). \tag{2.58}$$

More mathematical details on these families can be found in [6].

To obtain exact solution of (2.56) and (2.57) for various real scenarios, the numerical solution of the free boundary problem (with a conventional equilibrium solver) and subsequent projection of the numerically obtained solution onto the exact solutions via a least squares fitting procedure is implemented [6]. The obtained solution can be written in the form

$$\begin{aligned}\psi = {} & c_1 + c_2 r^2 + rJ_1(pr)(c_3 + c_4 z) + c_5 \cos pz + c_6 \sin pz + \\ & + r^2(c_7 \cos pz + c_8 \sin pz) + c_9 \cos p\sqrt{r^2 + z^2} + \\ & + c_{10} \sin p\sqrt{r^2 + z^2} + rJ_1(vr)(c_{11} \cos qz + c_{12} \sin qz) + \\ & + rJ_1(qr)(c_{13} \cos vz + c_{14} \sin vz) + \\ & + rY_1(vr)(c_{15} \cos qz + c_{16} \sin qz) + \\ & + rY_1(qr)(c_{17} \cos vz + c_{18} \sin vz),\end{aligned} \tag{2.59}$$

where corresponding vector of coefficients $c_i$ can be found in [6].

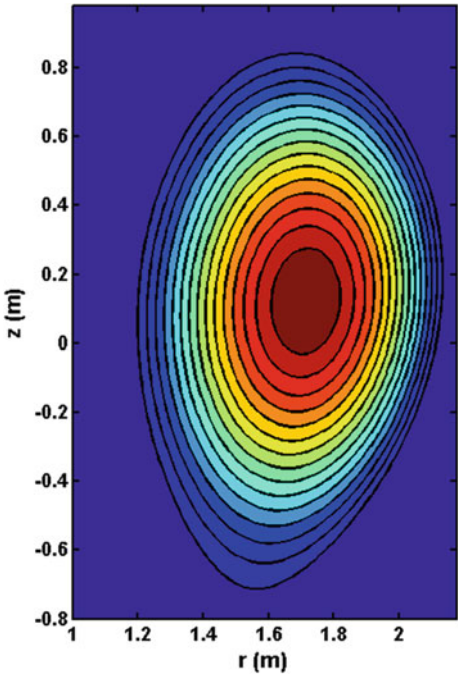


**Fig. 2.10** Exact GSE solution for ASDEX Upgrade discharge # 10 958, $t = 5.20\,\mathrm{s}$

### *2.5.5 Computational Example*

Computational example depicted in Fig. 2.10 corresponds to the results for tokamak equilibrium obtained using analytical solution (2.59). The highest value for the poloidal magnetic flux $\psi_{max} = 1.4\,\mathrm{Tm}^2$ is observed at the center of tokamak plasma, as it is expected, while the final contour (called separatrix) defines the area where the value of the magnetic flux is equal to zero.

## 2.6 Concluding Remarks

In the paper, some analytical methods for solving various integro-differential equationss in electromagnetic compatibility have been reviewed. Of particular interest are thin wire configurations buried in a lossy medium. Both frequency and time domain solutions are considered. Solutions in the frequency domain are obtained by performing certain mathematical manipulations with the unknown current function. On the other hand, solutions in the time domain are carried out using the Laplace transform and Cauchy residue theorem. The trade-off between the presented methods is given in this review paper, as well. Obtained analytical results are compared to

those calculated by means of various numerical solutions, where applicable. Finally, an overview of well-established and widely used analytical solutions of the Grad–Shafranov equation is given and discussed.

## References


1. Ambrosino, G., Albanese, R.: Magnetic control of plasma current, position, and shape in Tokamaks: A survey or modeling and control approaches. IEEE Control Syst. **25**, 76–92 (2005)
2. Atanasiu, C.V., Günter, S., Lackner, K., Miron, I.G.: Analytical solutions to the Grad–Shafranov equation. Phys. of Plasmas (1994-present) **11**, 3510–3518 (2004)
3. Barnes, P.R., Tesche, F.M.: On the direct calculation of a transient plane wave reflected from a finitely conducting half space. IEEE Trans. Electromagn. Compat. **33**, 90–96 (1991)
4. Bogerd, J.C., Tijhuis, A., Klaasen, J.J.A.: Electromagnetic excitation of a thin wire: A traveling-wave approach. IEEE Trans. Antennas Propag. **46**, 1202–1211 (1998)
5. Bridges, G.E.J.: Fields generated by bare and insulated cables buried in a lossy half-space. IEEE Trans. Geosci. Remote Sens. **30**, 140–146 (1992)
6. Carthy, P.J.M.: Analytical solutions to the Grad-Shafranov equation for tokamak equilibrium with dissimilar source functions. Phys. of Plasmas (1994-present) **6**, 3554–3560 (1999)
7. Grcev, L., Dawalibi, F.: An electromagnetic model for transients in grounding systems. IEEE Trans. Power Deliv. **5**, 1773–1781 (1990)
8. Hoorfar, A., Chang, D.: Analytic determination of the transient response of a thin-wire antenna based upon an SEM representation. IEEE Trans. Antennas Propag. **30**, 1145–1152 (1982)
9. King, R.W.P.: Embedded bare and insulated antennas. IEEE Trans. Biomed. Eng. **BME–24**, 253–260 (1977)
10. King, R.W.P., Fikioris, G.J., Mack, R.B.: Cylindrical Antennas and Arrays. Cambridge University Press, UK (2002)
11. Miller, E.K., Poggio, A.J., Burke, G.J.: An integro-differential equation technique for the time-domain analysis of thin wire structures. I. The numerical method. J. of Computational Phys. **12**, 24–48 (1973)
12. Poljak, D.: Advanced Modeling in Computational Electromagnetic Compatibility. Wiley, New Jersey (2007)
13. Poljak, D., Doric, V.: Wire antenna model for transient analysis of simple grounding systems, Part I: The vertical grounding electrode. Prog. In Electromagn. Res. **64**, 149–166 (2006)
14. Poljak, D., Doric, V.: Wire antenna model for transient analysis of simple grounding systems, Part II: The horizontal grounding electrode. Prog. In Electromagn. Res. **64**, 167–189 (2006)
15. Poljak, D., Kovac, N.: Time domain modeling of a thin wire in a two-media configuration featuring a simplified reflection/transmission coefficient approach. Eng. Anal. with Bound. Elem. **33**, 283–293 (2009)
16. Poljak, D., Doric, V., Rachidi, F., Drissi, K., Kerroum, K., Tkachenko, S.V., Sesnic, S.: Generalized form of telegrapher's equations for the electromagnetic field coupling to buried wires of finite length. IEEE Trans. on Electromagn. Compat. **51**, 331–337 (2009)
17. Poljak, D., Sesnic, S., Goic, R.: Analytical versus boundary element modelling of horizontal ground electrode. Eng. Anal. with Bound. Elem. **34**, 307–314 (2010)
18. Rao, S.M.: Time Domain Electromagnetics. Academic Press, Cambridge (1999)
19. Schiff, J.L.: The Laplace Transform: Theory and Applications. Springer, Heidelberg (1999)
20. Sesnic, S., Poljak, D.: Antenna model of the horizontal grounding electrode for transient impedance calculation: Analytical versus boundary element method. Eng. Anal. with Bound. Elem. **37**, 909–913 (2013)
21. Sesnic, S., Poljak, D., Tkachenko, S.V.: Time domain analytical modeling of a straight thin wire burried in a lossy medium. Prog. In Electromagn. Res. **121**, 485–504 (2011)

22. Sesnic, S., Poljak, D., Tkachenko, S.V.: Analytical modeling of a transient current flowing along the horizontal grounding electrode. IEEE Trans. on Electromagn. Compat. **55**, 1132–1139 (2013)
23. Takashima, T., Nakae, T., Ishibashi, R.: Calculation of complex fields in conducting media. IEEE Trans. on Electr. Insul. **EI–15**, 1–7 (1980)
24. Tijhuis, A., Zhongqiu, P., Bretones, A.: Transient excitation of a straight thin-wire segment: A new look at an old problem. IEEE Trans. on Antennas and Propag. **40**, 1132–1146 (1992)
25. Tkatchenko, S., Rachidi, F., Ianoz, M.: Electromagnetic field coupling to a line of finite length: theory and fast iterative solutions in frequency and time domains. IEEE Trans. on Electromagn. Compat. **37**, 509–518 (1995)
26. Tkatchenko, S., Rachidi, F., Ianoz, M.: High-frequency electromagnetic field coupling to long terminated lines. IEEE Trans. on Electromagn. Compat. **43**, 117–129 (2001)
27. Velazquez, R., Mukhedkar, D.: Analytical modelling of grounding electrodes transient behavior. IEEE Trans. Power Appar. Syst. **PAS–103**, 1314–1322 (1984)
28. Zheng, S.B., Wootton, A.J., Solano, E.R.: Analytical tokamak equilibrium for shaped plasmas. Phys. of Plasmas (1994-present) **3**, 1176–1178 (1996)

http://www.springer.com/978-3-319-42081-3

Engineering Mathematics I
Electromagnetics, Fluid Mechanics, Material Physics
and Financial Engineering
Silvestrov, S.; Rančić, M. (Eds.)
2016, XV, 341 p. 135 illus., 67 illus. in color., Hardcover
ISBN: 978-3-319-42081-3